Biosensors and Bioelectronics 160 (2020) 112206

Contents lists available at ScienceDirect

Biosensors and Bioelectronics

journal homepage: http://www.elsevier.com/locate/bios

Conformal, waterproof electronic decals for wireless monitoring of sweat and vaginal pH at the point-of-care

Aniket Pal [a], Vinayak G. Nadiger [a], Debkalpa Goswami [a], Ramses V. Martinez [a,b,*]

[a] School of Industrial Engineering, Purdue University, 315 N. Grant Street, West Lafayette, IN, 47907, USA
[b] Weldon School of Biomedical Engineering, Purdue University, 206 S. Martin Jischke Drive, West Lafayette, IN, 47907, USA

ARTICLE INFO

Keywords:
Wearable electronic decals
Sweat pH sensor
Vaginosis detection
Wireless monitoring
Waterproof flexible biosensor
Impedance spectroscopy
Point-of-care testing

ABSTRACT

While the monitoring of pH has demonstrated to be an effective technique to monitor an individual's health state, the design of wearable biosensors is subject to critical challenges, such as high fabrication costs, thermal drift, sensitivity to moisture, and the limited applicability for users with metal allergies. This work describes the low-cost fabrication of waterproof electronic decals (WPEDs): highly conformable disposable biosensors capable of monitoring sweat and vaginal pH. WPEDs contain a polyaniline/silver microflakes sensing layer optimized for accurate impedance-based pH quantification across the clinically relevant range of variation of most biofluids. WPEDs also contain a heating layer that serves to both stimulate sweating and prevent saturation of the sensing area, reducing the variability of the measurements. The conformability of WPEDs enables their simple and allergy-free attachment to skin, where they can monitor sweat pH, or to the surface of paper-based sample containers, for the pH-based diagnosis of bacterial vaginosis. WPEDs are mostly transparent, self-adhesive, breathable, flexible, moisture-insensitive, and able to maintain their accuracy under significant mechanical and thermal stresses. A cost-effective wearable and portable impedance analyzer wirelessly transmits pH data in real-time to the smartphone of the user, where a custom-developed App enables long term monitoring and telemedicine applications. Our results demonstrate the feasibility of using inexpensive single-use WPEDs and a reusable, wireless impedance analyzer to provide a wearable solution for the real-time monitoring of sweat pH and the accurate at-home diagnosis of bacterial vaginosis, improving the capabilities of current low-cost, point-of-care diagnostic tests.

1. Introduction

The development of flexible and wearable electronic biosensors has garnered considerable attention due to their potential to provide early diagnosis and monitor an individual's health state. Most of the initial wearable sensors focused on monitoring physiological signals such as breathing and heart rates, temperature, or muscular activity due to their simple acquisition methods (Bandodkar et al., 2015). The recent development of wearable chemical sensors has demonstrated the non-invasive quantification of a variety of biomarkers on sweat and tears (Bariya et al., 2018; Fay et al., 2012; Koh et al., 2016; La Belle et al., 2016; Yao et al., 2011). Unfortunately, the cost of these wearable chemical sensors is often too high for single-use applications, especially for at-home testing or point-of-care diagnostics, due to the costly materials and manufacturing techniques required for their fabrication, as well as the expensive electronics required to acquire the measurements (Gao et al., 2016; Koh et al., 2016; La Belle et al., 2016; Morris et al., 2009; Yao et al., 2011). Here, we propose an inexpensive method to fabricate conformable electronic decals comprising a thermal stimulator and a flexible biosensor capable of monitoring the pH of most biofluids. The simple interfacing between these single-use electronic decals and a reusable wireless impedance analyzer enables the use of these biosensors for the point-of-care monitoring of sweat pH and the at-home monitoring of vaginal pH to detect vaginal infections.

Sweat contains a variety of analytes relevant for the assessment of the biomolecular state of an individual (Bariya et al., 2018). Sweat pH is particularly attractive as it is related to the concentration of different electrolytes and serves as an indicator for dehydration (Sonner et al., 2015), metabolic activity (Morris et al., 2009), and several diseases, such as cystic fibrosis (Desax et al., 2008; Wu et al., 2017), dermatitis (Schmid-Wendtner and Korting, 2006), or alkalosis (Patterson et al., 2002). Additionally, pH monitoring of vaginal fluid has been

* Corresponding author. School of Industrial Engineering, Purdue University, 315 N. Grant Street, West Lafayette, IN, 47907, USA.
E-mail address: rmartinez@purdue.edu (R.V. Martinez).

https://doi.org/10.1016/j.bios.2020.112206
Received 17 January 2020; Received in revised form 24 March 2020; Accepted 9 April 2020
Available online 17 April 2020

demonstrated to be an effective way to provide early diagnosis of bacterial vaginosis (BV) (Hemalatha et al., 2013). Unfortunately, while rapid test strips have been developed to identify BV, their limited accuracy impedes early diagnosis and only allows the proper identification of BV after significant bacterial proliferation (Hemalatha et al., 2013; Khandalavala and Van Geem, 1999).

To decrease the cost of wearable chemical sensors, several portable and on-skin colorimetric tests have been proposed using disposable microfluidic devices (Caldara et al., 2016; Choi et al., 2019; Koh et al., 2016). Wearable sweat tests are often fabricated using low-cost substrates such as textile (Caldara et al., 2016; Morris et al., 2009; Parrilla et al., 2016) or thin silicone layers (Koh et al., 2016) and rely on the capillary filling of sensing zones containing reagents that change color depending on the concentration of their target biomarker. These devices, however, have limited resolution and cannot provide continuous or hands-off measurements. To address these limitations, several wireless potentiometric and amperometric sensors have demonstrated the accurate transduction of their electrochemical interaction with analytes into voltage or current signals (Bandodkar et al., 2013; Guinovart et al., 2014; Novell et al., 2012; Oh et al., 2018; Parrilla et al., 2016; Rahimi et al., 2017). Electrochemical sensors, however, require complex electronics that are often difficult to miniaturize into cost-effective wearable systems. Additionally, potentiometric sensors have a limited resolution for pH (~55 mV/pH) (Bandodkar et al., 2013; Guinovart et al., 2014; Oh et al., 2018; Rahimi et al., 2017), impeding the accurate detection of small variations of pH for most biofluids across their clinically relevant physiological range (3–8.5) (Huang et al., 2011; Novell et al., 2012; Rahimi et al., 2016). Electrical chemical sensors have recently demonstrated to provide a sensing resolution and accuracy similar to electrochemical sensors using relatively simple and easy-to-miniaturize measuring electronics, facilitating their use as wearable sensors (Kassal et al., 2018). These sensors rely on the change of their electrical properties, such as capacitance or resistance, when in contact with the target analyte. The prolonged use of these sensors on skin, however, can lead to irritation and allergies due to their limited breathability and the constant contact between skin and metals. Furthermore, environmental moisture, variations in temperature, and the saturation of the sensing area often increase the variability of measurements of electrical chemical sensors, compromising their accuracy.

Latest advances in wireless communication (RFID, NFC, BLE) have facilitated the development of reusable reading and display platforms that significantly simplify the electronics of the wearable chemical sensor, reducing their overall cost (Pal et al., 2018, 2017). These passive wearable sensors, however, exhibit relatively short read ranges (from few cm to several meters), limiting the motion of the user.

Our previous work in wearable electrochemical sensors demonstrated the use of pH as a biomarker to monitor chronic wound infections (Pal et al., 2018). Here, we present waterproof electronic decals (WPEDs): highly conformable low-cost biosensors capable of monitoring pH levels across the clinically relevant range of variation of most biofluids. WPEDs can be easily mounted on skin to monitor sweat pH levels, or on the surface of paper-based sample containers to detect anomalies in the vaginal pH caused by bacterial vaginosis. The combination of WPEDs with a wireless impedance analyzer enables the accurate measurement of pH at the point of care. WPEDs also offer several advantages as follows: (i) Their flexibility, conformability, and breathability eliminate their somatosensory perception; (ii) their simple manufacturing and low cost (~0.08 USD) enable their use as disposable, single-use diagnostic devices; (iii) their hydrophobic outer surface eliminates the variability of the acquired measurements due to environmental moisture; (iv) the reusable wireless measurement and communication system enables the wearable monitoring of sweat pH and the at-home detection of vaginal infections.

2. Materials and methods

2.1. Chemicals and instrumentation

We purchased two conductive inks, Ag/AgCl (AGCL-675) and carbon (C-200), from Applied Ink Solutions. We procured silver microflakes (AgμF, particle size 2–5 μm) from Inframat Advanced Materials LLC. Polyaniline emeraldine base (PANi-EB, Mw = 50 kDa), ethyl cellulose (EC, 48.0% ethoxyl basis), poly(dimethylsiloxane) (PDMS, SYLGARD-184), poly(vinyl alcohol) (PVA, 4% aqueous solution), ethanol (C_2H_5OH), hydrochloric acid (HCl), disodium phosphate (sodium hydrogen phosphate), and citric acid (2-hydroxypropane-1,2,3-tricarboxylic acid) were purchased from Sigma Aldrich Inc. To render cellulose-based paper (Whatman #1, GE Healthcare Inc) omniphobic, a 4.76% v/v solution of trichloro(3,3,4,4,5,5,6,6,7,7,8,8,9,9,10,10,11,11,12,12,12 henicosafluorododecyl)silane ("$C^{12}F$", from Gelest Inc.) in isopropanol was used as fluoroalkylated silanizing agent. We used a commercial, benchtop potentiostat (Reference 3000; Gamry Instruments Inc.) to test the performance of the WPEDs and the wearable impedance analyzer. All thermal infrared (TIR) images were captured using a handheld thermal camera (FLIR-E8, thermal sensitivity = 0.05 °C, FLIR Inc.)

2.2. Fabrication of the wearable and portable impedance analyzers

We fabricated a wearable impedance analyzer using an integrated circuit capable of performing electrical impedance spectroscopy (AD5933, Analog Devices Inc.) controlled by a Wi-Fi enabled microcontroller (Photon, Particle Inc.). The impedance analyzer is powered by a rechargeable lithium-ion battery (LP401230, Adafruit Industries LLC). The microcontroller uses an in-built Wi-Fi module (BCM43362, Cypress Semiconductor Corp.) for wireless communication on the 802.11 b/g/n band. The electronic components of the wearable impedance analyzer were mounted on a flexible printed circuit board and housed inside a wearable cotton sweatband (Suddora LLC) or a portable 3D printed housing (Form 2 SLA, FormLabs Inc.). To interface the impedance analyzer to the WPED, we embroidered connectors and contact pads using conductive fabric thread (Lyofil 166, Uniqe Aviation Inc.).

2.3. Fabrication of WPEDs for pH sensing

We created a decal transfer substrate by spraying a ~50-μm-thick layer of PVA on a sheet of calendered paper (ELE-300, Elements Inc.) and allowing it to dry at room temperature. We made a 2.5% (w/w) solution of EC in ethanol and added PDMS prepolymer to this solution in a 5% (w/w) concentration, stirring the mixture for 10 min until full dispersion was achieved. The EC/PDMS ethanolic solution was then spin-coated over the PVA layer of the transfer substrate at 1000 rpm for 40 s. After curing the transfer substrate at 60 °C for 2 h, the ethanol evaporated leaving a ~10-μm-thick transparent layer of EC/PDMS coating the PVA layer. We stencil printed two flexible, parallel electrodes on the EC/PDMS layer using Ag/AgCl ink and coated the region between the parallel electrodes with carbon ink to create a resistive heating element (Figs. S1 and S2). We encapsulated the heating element by spin coating a 2.5% (w/w) EC solution in ethanol at 1000 rpm for 30 s. On top of this ~10-μm-thick EC layer, we stencil printed two flexible parallel electrodes smaller than those printed on the EC/PDMS layer. We created a conductive polymeric composite by mixing 150 mg of a pH responsive polymer (PANi-EB) with 300 mg of AgμF in 5 mL of isopropyl alcohol (IPA) and sonicated the mixture for 2 h to achieve a uniform suspension. A 15 μL drop of this blue-colored, pH-sensitive suspension was used to coat the region between the parallel electrodes. After curing the PANi-EB/AgμFs at 60 °C for 30 min, we doped it by exposing it to HCl vapors in a desiccator at 36 Torr for 30 min. The diffusion of the H+ ions (doping agents) from the HCl vapor into the blue-colored PANi-EB of the PANi/AgμFs composite transforms it into a

green-colored PANi-ES (polyaniline emeraldine salt, Fig. S6), which exhibits a higher conductivity (~10^8 S/m) than the PANi-EB form (~10 S/m) (Sukitpaneenit et al., 2007). The PANi-ES/AgμFs composite and the Ag/AgCl electrodes were coated with 20 μL of a 2.5% (w/w) solution of EC in aqueous ethanol (65% w/w), which, after drying at room temperature, created a hydrophilic, 50-μm-thick, porous ethyl cellulose (p-EC) layer (Fig. S3).

2.4. Calibration of the WPEDs

To calibrate the WPEDs, we prepared McIlvine buffers with pH ranging 2.8–8.6 by mixing a 0.2 M solution of disodium phosphate and a 0.1 M solution of citric acid in different ratios (Pearse, 1968) (Table S1). A commercial pH meter (Model IQ125, IQ Scientific Instruments) was used to verify the pH of each McIlvine buffer. To find a relationship between the impedance of the PANi/AgμFs composite and the environmental pH level, we pipetted 10 μL of the different McIlvaine buffers on nine different WPEDs and performed impedance spectroscopy by applying sinusoidal signals with an amplitude of 100 mV and frequencies ranging 10 Hz–100 kHz using a commercial, benchtop potentiostat.

2.5. Wireless pH monitoring of sweat and vaginal fluid using WPEDs

On-skin sweat pH measurements were collected from the forearms of an exercising volunteer using WPEDs. Sweatband-like impedance analyzers worn on each arm were used to interface the WPEDs and collect and wirelessly transmit the sweat pH measurements. To enhance sweat production, the skin of the participant was thermally stimulated by locally applying heat (38.5 °C) with the heating element of the WPED. Sweat pH measurements were collected along each of the phases of a 1-h workout (at rest, high, moderate, and low intensity exercise). To monitor the pH of vaginal fluid, we created a portable WPED-based device comprising two components: A re-usable measuring base containing a wireless impedance analyzer and a single-use omniphobic paper-based sample container with a WPED attached to its bottom. A female volunteer out of her menstrual cycle collected vaginal fluid in a tampon by wearing it for 3–5 h. After its removal, the tampon was placed over the WPED, on the omniphobic paper container, and this container was placed on the measuring base during 5 min. The collected

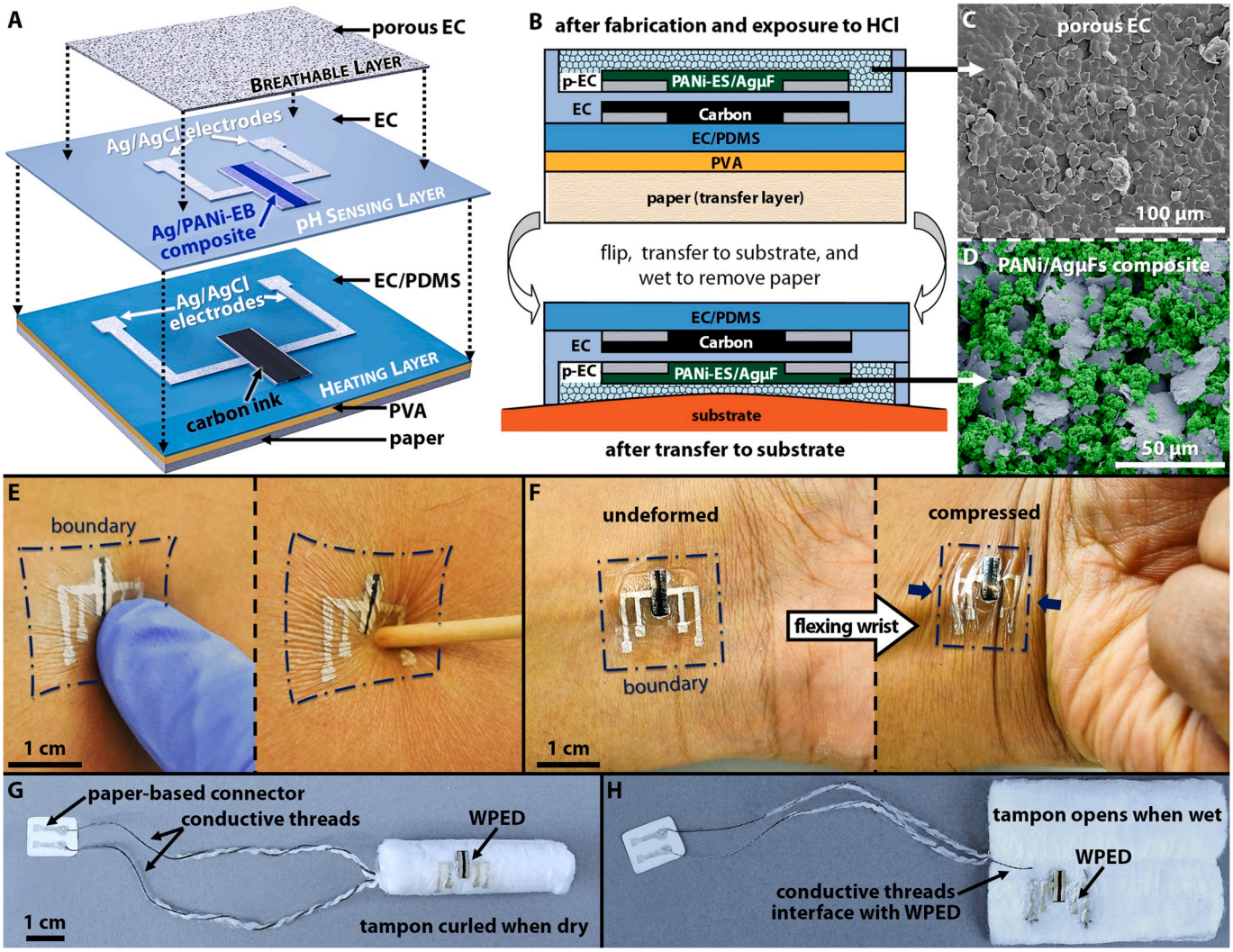

Fig. 1. WPED fabrication process and its integration onto skin and sanitary tampons. (A) Schematics of the multilayered structure of the WPED. (B) Schematics of the cross-section of the WPED, before and after its transfer to a measuring platform. (C, D) Scanning electron microscopy images of the porous EC layer (top) and the PANi/AgμF composite (bottom). (E) WPED withstanding mechanical stresses after being transferred onto skin. (F) WPED transferred onto skin, undergoing flexion. The dashed line shows the boundary of the WPED. (G, H) WPEDs mounted on sanitary tampons for the detection of BV by monitoring the pH of vaginal fluid. WPEDs remain conformally attached to the tampon even after their expansion due to fluid absorption. Two conductive threads coiled around the strings of the tampon and coated with PDMS are secured to the WPED on one end and to the flexible paper-based connector on the other end using epoxy.

measurement of vaginal pH was then wirelessly transmitted to a laptop computer (Figs. S4 and S5). After the test is performed, the paper-based container holding both the tampon and the WPED can be easily disposed, facilitating the cleaning of the wireless measuring stage.

3. Results and discussion

3.1. pH sensing using WPEDs

Fig. 1A shows the exploded view of a WPED, which comprises three different layers: (i) a breathable p-EC layer (Figs. 1B, C, S9), which can be easily attached to a variety of deformable surfaces (such as the skin of the user or other cellulose-based materials) and is capable of driving biofluids from its surface to the pH sensing layer; (ii) a pH sensing layer containing the PANi/AgμFs composite (Fig. 1D) and two Ag/AgCl electrodes printed on EC; (iii) a heating layer with a resistive heating element that stimulates sweating and, prior to collecting the pH measurement, dries the pH sensing area to reduce the variability of the measurements (Niarchos et al., 2017). WPEDs are fabricated on top of a PVA coated paper substrate, which facilitates the manipulation and transfer of the electronic decal onto the measuring platform (Fig. 1B, top). To measure sweat pH, the WPED is placed on the skin of the user and the paper substrate is wetted with water, which dissolves the sacrificial PVA layer and releases the WPED on the skin of the user (Fig. 1B, bottom). The low thickness of the WPED (~80 μm) and the hydrophilic behavior of the p-EC layer in contact with the skin of the user readily secure the electronic decal to the skin of the user without requiring any glue layer to prevent delamination (Fig. 1E). Additionally, WPEDs readily conform to the surface of the skin without constraining the natural movements of the wearer (Fig. 1F), eliminating the somatosensory perception of these electronic decals. Forearms and calves are ideal locations for attaching WPEDs, since they facilitate interfacing with the wearable impedance analyzer housed in sweatband and minimize the stretching of the WPEDs.

To measure the pH of unknown buffer solutions, WPEDs can be attached to any conventional sanitary tampon (Fig. 1G). The hydrophilic cellulose fibers of the sanitary tampon act as a coarse filter for the solution and enable the uniform wetting of the WPED. The flexibility, small thickness, and self-adhesion of the WPEDs facilitate their firm attachment to the surface of the tampon even after its significant expansion due to fluid saturation (Fig. 1H). After removing the tampon from the unknown solution, the heating layer of the WPED dries the sensing layer prior to the collection of a pH measurement using a wearable or portable impedance analyzer (Fig. 2).

To effectively stimulate sweating (Benjamin, 1953), the heating element of the WPED applies a localized heat stress (38.5 °C for 3 min) on the skin of the user. The microporous structure of the EC layer drives biofluids in contact with it (Fig. 1C) to the pH sensing layer by capillary action. Additionally, the small pore size (~0.5–1.0 μm) of the EC layer prevents the metals of the measuring electrodes or the sensing layer from coming in direct contact with the skin of the user, avoiding irritation and allergic reactions for users sensitized to metals. The

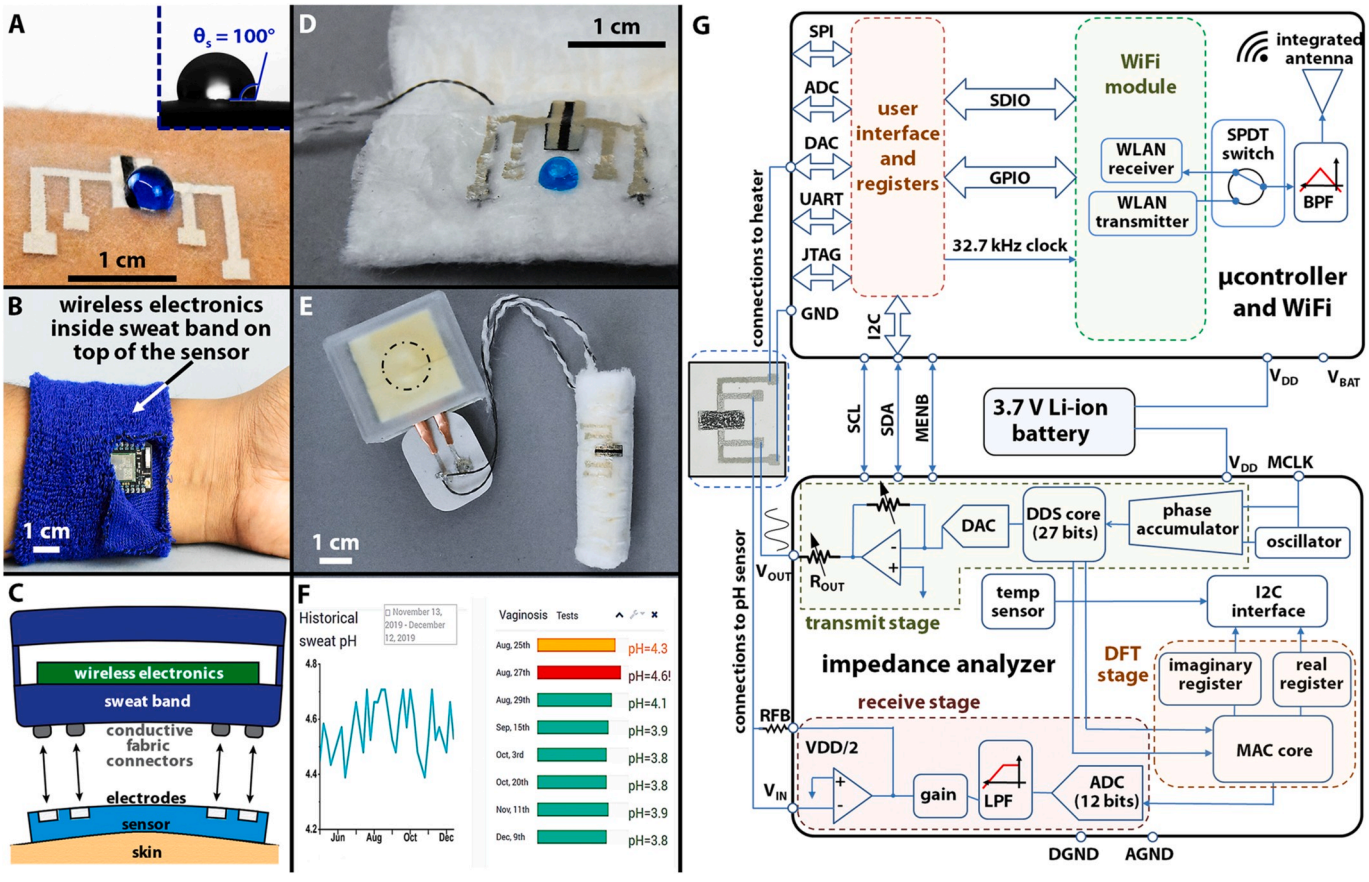

Fig. 2. Wearable and portable impedance analyzers for wireless pH monitoring. (A) Transparent, hydrophobic EC/PDMS layer encapsulating the WPED. Inset shows a static contact angle (θ_s) of 100° with water. (B) Incorporation of the impedance analyzer inside a sweatband, which is worn on top of the WPED to monitor sweat pH. (C) Schematics showing the interfacing between the wearable impedance analyzer and a WPED through embroidered conductive fabric connectors. (D) WPED mounted on a sanitary tampon. (E) Portable impedance analyzer capable of measuring the pH of unknown solutions by interfacing with a tampon-mounted WPED. This portable impedance analyzer measures and transfers pH data after the user pushes its top button (circled) (F) Mobile App developed to receive, display, store, encrypt, and transmit the results. (G) Schematics of the electronics in the wireless impedance analyzer used to monitor pH using WPEDs. Test parameters and measured pH data are transferred wirelessly via Wi-Fi.

biocompatibility of PANi (Sun et al., 2016) and the antibiofouling properties of silver (Pietrzak et al., 2016) also ensure that WPEDs are consistent with epidermal applications. Once a fluid reaches the PANi/AgμFs sensor, the pH of the fluid regulates the relative equilibrium between the PANi-ES and PANi-EB states via H+ exchange, proportionally modifying its conductivity, and allowing us to correlate the changes in impedance of the PANi/AgμFs composite to the pH value (supplementary information S6). Most biofluids, as ionic aqueous solutions (Montain et al., 2007), are good conductors of electricity and can compromise the accuracy of the impedance-based sweat pH monitoring by short-circuiting the electrodes of the sensor, especially after long monitoring sessions. To maximize the stability of the pH sensor and enable reliable monitoring of pH over long periods of time, the heating element over the pH sensor (Fig. 1B) evaporates the analyte that has reacted with the PANi/AgμFs composite, preventing any short-circuit. The fluid evaporated at the pH sensing area is released to the atmosphere through the porous structure of the breathable p-EC layer and the gas permeable EC layer (supplementary section S4). Only after the heating layer completes the drying of the sensing area, is the pH measurement collected. The outermost layer of the WPED is a transparent EC/PDMS film which protects the WPED from environmental moisture and during water immersion due to the hydrophobic properties of the PDMS (Fig. 2A, D) (McDonald et al., 2000).

3.2. Fabrication of wireless impedance analyzers

To interface with the electronic decal while it is mounted on the skin of the user, we fabricated a flexible impedance analyzer circuit and embedded it between the textile layers of a highly conformable sweatband. This wearable impedance analyzer enables the wireless collection and transmission of pH measurements using WPEDs without causing significant constraints to the natural movements of the wearer. The sweatband conforms to the wrist of the user, facilitating the interface between the impedance analyzer circuit and the WPED using embroidered conductive fabric connectors (Fig. 2B and C). To measure the pH of unknown solutions or to monitor pH levels of vaginal fluid, the components of this impedance analyzer were placed on portable 3D-printed cases that simplify their interfacing with WPEDs.

The impedance analyzer comprises an impedance spectrometer IC, programed and controlled by a Wi-Fi enabled microcontroller, powered by a rechargeable 3.7 V Li-ion battery (Fig. 2D). The microcontroller also controls the resistive heating element in the WPED. The pH measurements are transmitted by Wi-Fi to the user's phone, where an App which we developed displays and stores the information (Fig. 2F, Figs. S4 and S5). Additionally, if the pH measurements are outside the clinically normal range, the App encrypts and transfers the data to relevant care givers (Pal et al., 2017).

The low cost of the WPEDs (~0.08 USD, see Table S2) ensures that they can be deployed as single-use devices. After sweat pH monitoring, the user can delaminate one corner of the WPED with their nails and peel off the whole device (without causing skin irritation) and dispose it. Upon incineration, WPEDs generate minimal amounts of solid byproducts (Fig. S10). While the WPEDs are single-use devices, the miniaturized impedance analyzer circuit (~26 USD, see Table S3) can be reused multiple times with different WPEDs and by different users.

3.3. Electrical performance of the PANi/AgμFs composite

Although the pH-responsive properties of PANi are well known (Rahimi et al., 2017, 2016), its resistance in the PANi-EB form is too high (~50 MΩ for the dimensions of the WPED) to be measured accurately, hampering the development of wearable, impedance-based pH sensors using PANi. To overcome this drawback, we optimized a PANi-based polymer composite previously developed by our team (Pal et al., 2018) to accurately measure pH over the clinical range of variation of most biofluids (sweat (Nyein et al., 2016): 5.5–7.5, vaginal fluid (King and Brucker, 2010): 3.8–4.5, wound exudate (Ochoa et al., 2014; Rahimi et al., 2016): 5.5–8.5, gastroesophageal reflux (Frazzoni et al., 2017): 3.0–7.0, urine (Rose et al., 2015): 5.5–7.0). In this work, we enrich the PANi-ES polymer with 200% (w/w) AgμFs. The high surface area and random orientation of the AgμFs enable the formation of efficient charge percolation networks through the PANi/AgμFs matrix, reducing its resistance to values (<10 MΩ) that can easily be measured using inexpensive, miniaturized instrumentation.

To characterize the changes in the impedance of the PANi/AgμFs composite due to changes in environmental pH, we exposed the WPED to various pH buffers (2.8–8.6) and measured their complex impedances across a broad range of frequencies (1 Hz–1 MHz). Fig. 3A shows the dependence of the resistance (real component of the complex impedance) on the frequency for WPEDs exposed to different pH levels. The proposed PANi/AgμFs composite exhibits minimal dielectric dispersions at low pH values, since the concentration of AgμFs efficiently reduced the dielectric behavior of PANi. Even for high pH values (6–8), dielectric dispersions only appear at frequencies greater than 100 kHz, demonstrating that the PANi/AgμFs composite remains sensitive to pH changes over a larger frequency range than that of pure PANi (Lee et al., 1993; Singh et al., 1999; Soares et al., 2006). The reactance spectra (imaginary component of the complex impedance) shows a single peak at high frequencies (Fig. 3B). The shifting to higher frequencies of these reactance peaks, as well as their reduction in amplitude when acidity is increased, can be explained by the faster charge transfer in the protonated PANi-ES/AgμFs composite. The increasing negative phase angles (Fig. 3C) at higher pH values show the increasing capacitive character of the PANi/AgμFs composite as the conductivity of the PANi decreases. The Nyquist plots of the PANi/AgμFs composite shown in Fig. 3D exhibit a single arc (in agreement with the single reactance peak), demonstrating that there is a single relaxation time for the frequencies being considered. We hypothesize that the incorporation of AgμFs to the PANi matrix shifted the second (weak) relaxation peak of PANi (Lee et al., 1993; Singh et al., 1999; Soares et al., 2006) to frequencies higher than the range used to operate the PANi/AgμFs pH sensor, enhancing the stability of the pH values measured by WPEDs.

3.4. Thermal performance of the sweat stimulator

The heating layer of the WPEDs (Fig. 1A) contains a resistive heating element lying on top of the PANi/AgμFs based pH sensor, separated by a non-conductive layer of EC. Fig. 4A shows TIR images of an on-skin WPED with the active heating element in OFF and ON conditions. Prior to collecting a pH measurement, the heating layer of the WPED is activated, which locally increases the temperature of the underlying skin up to (38.5 °C, see Fig. 4A). This increase in temperature, stimulates the production of sweat up to 180 μL/cm^2/hour (Bariya et al., 2018; Wingo et al., 2010). This sweat rapidly wicks through the p-EC layer helped by capillary action and reaches the sensing layer of the WPED. Fig. 4D shows how, after the sensing layer is wetted, the thermal layer requires to be active for a certain amount of time (3–15 min, depending on the volume of liquid to evaporate) until the evaporation rate exceeds the sweating rate of the user, drying the PANi/AgμF composite. Only after the sensing layer is completely dry, is the pH measurement is collected, which ensures that the measured impedance corresponds to the interaction between the pH of the biofluid being measured and the PANi/AgμFs composite. Additionally, the evaporation of the analyte from the pH sensing layer prevents the electrodes from being short-circuited. Since the heater is separated from the pH sensor by an ~10-μm-thick layer of EC, the temperature at the PANi/AgμFs composite reaches a steady state in ~10 s (Fig. 4B). The temperature at the pH sensor can be controlled by tuning the voltage applied to the resistive element of the heating layer. Fig. 4C shows the control and repeatability of the temperatures induced at the sensing layer over multiple heating cycles as well as its rapid cooling due to the efficient heat dissipation of WPEDs. We characterized the performance of the heaters by soaking the pH

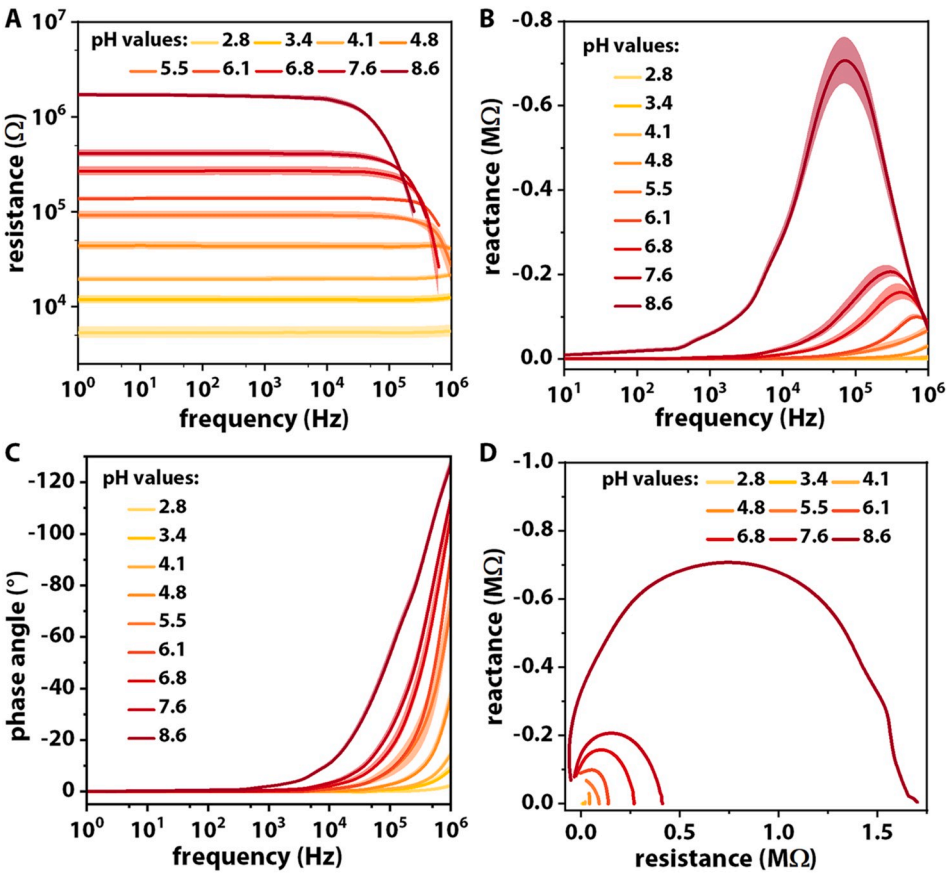

Fig. 3. Electrical performance of the pH sensitive layer of the WPEDs. (A, B, C) Dependence of the resistance (A), reactance (B), and phase (C) of the PANi/AgμFs composite on the reading frequency at different pH levels (2.8–8.6) (D) Nyquist plot of the PANi/AgμFs composite.

sensors with water and maintaining the heater at different temperatures until complete evaporation. During the application of heat, the wearable impedance analyzer continuously monitors the resistance of the pH sensor, identifying its drying to be complete when the increments in resistance become smaller than 5% in 30 s. We characterized the drying time of the pH sensor at different temperatures induced by the heating element of the WPED (Fig. 4D). WPEDs, when used as skin-mounted devices, dry after maintaining a wearer-safe constant temperature of 40 °C for 15 min. When used as *ex-vivo* pH sensors, WPEDs dry in only 3 min at 60 °C.

3.5. *Wireless monitoring of sweat and vaginal pH using WPEDs*

Fig. 5 shows how WPEDs, in combination with a wearable or portable impedance analyzer, can monitor pH levels of sweat or vaginal fluid. We first calibrate the impedance analyzers with pH buffers at a 10 kHz frequency to maximize the contrast between impedances due to pH values (Fig. 5A). Working frequencies higher than 10 kHz result in impedance values decreasing with frequency, especially at high pH levels, due to the capacitive effects exhibited at those frequencies by the PANi/AgμFs composite.

The impedance of the PANi/AgμFs composite depends on the relative composition of the two phases of PANi (PANi-EB and PANi-ES), which is regulated by the concentration of H+ ions. Since pH is defined as the decimal logarithm of the reciprocal of the H+ concentration, the logarithm of the impedance modulus exhibits a linear correlation with pH values (Fig. 5B). Therefore, we can describe the relationship between the modulus of the impedance and pH as: $\log_{10}|Z| = A + \beta \cdot$ pHwhere A and β are experimentally determined fitting parameters depending on the composition of the PANi/AgμFs composite and the design of the WPED (supplementary section S6). Using experimental results obtained at 10 kHz (indicated by the dashed line in Fig. 5B), we calibrated the pH sensing capabilities of WPEDs according to the following equation: $\log_{10}|Z| = 2.64 + 0.407 \cdot pH$ (Fig. 5B). This equation describes WPEDs across the 2.8–8.6 pH range, which covers the clinical range of variation of pH for vaginal fluid (King and Brucker, 2010) (3.8–4.5) and sweat (Nyein et al., 2016) (5.5–7.5).

Once we verified that WPEDs are able to accurately quantify pH levels of buffers, we tested their pH sensing performance with real biofluids. WPEDs were attached to each of the forearms of a volunteer and sweatband-like wearable impedance analyzers were used to monitor his sweat pH across the different phases of a 1-h workout (Fig. 5C and D). At rest, the sweat pH of the volunteer was ~6.3, which increased to ~7.2 during exercise (Fig. 5E). This increment in pH can be explained by the decrease of lactic acid concentration in sweat during exercise (Gao et al., 2016). All pH values measured by WPEDs were verified using a commercial pH tester.

Periodic vaginal pH monitoring enables the detection of BV (Hemalatha et al., 2013). We also demonstrate the use of WPEDs, in combination with a portable impedance analyzer, to monitor vaginal pH at home. This point-of-care testing device comprises two components: A re-usable measuring base containing a wireless impedance analyzer and a single-use omniphobic paper-based box with a WPED attached to its bottom (Fig. 5F). The electrical contacts of the WPED are folded so that they are in contact with the conductive pads printed on the measuring base, which enable the interfacing between the WPED and the impedance analyzer. We rendered the paper-box omniphobic using a fluoroalkyl organosilane ($C^{12}F$), following the experimental procedure described by our group in previous publications (Pal et al., 2018; Sala de Medeiros et al., 2019). Prior to collecting measurements of the vaginal pH, a healthy female volunteer out of her menstrual cycle wore a sanitary tampon for 5 h. The tampon was simply placed on the omniphobic

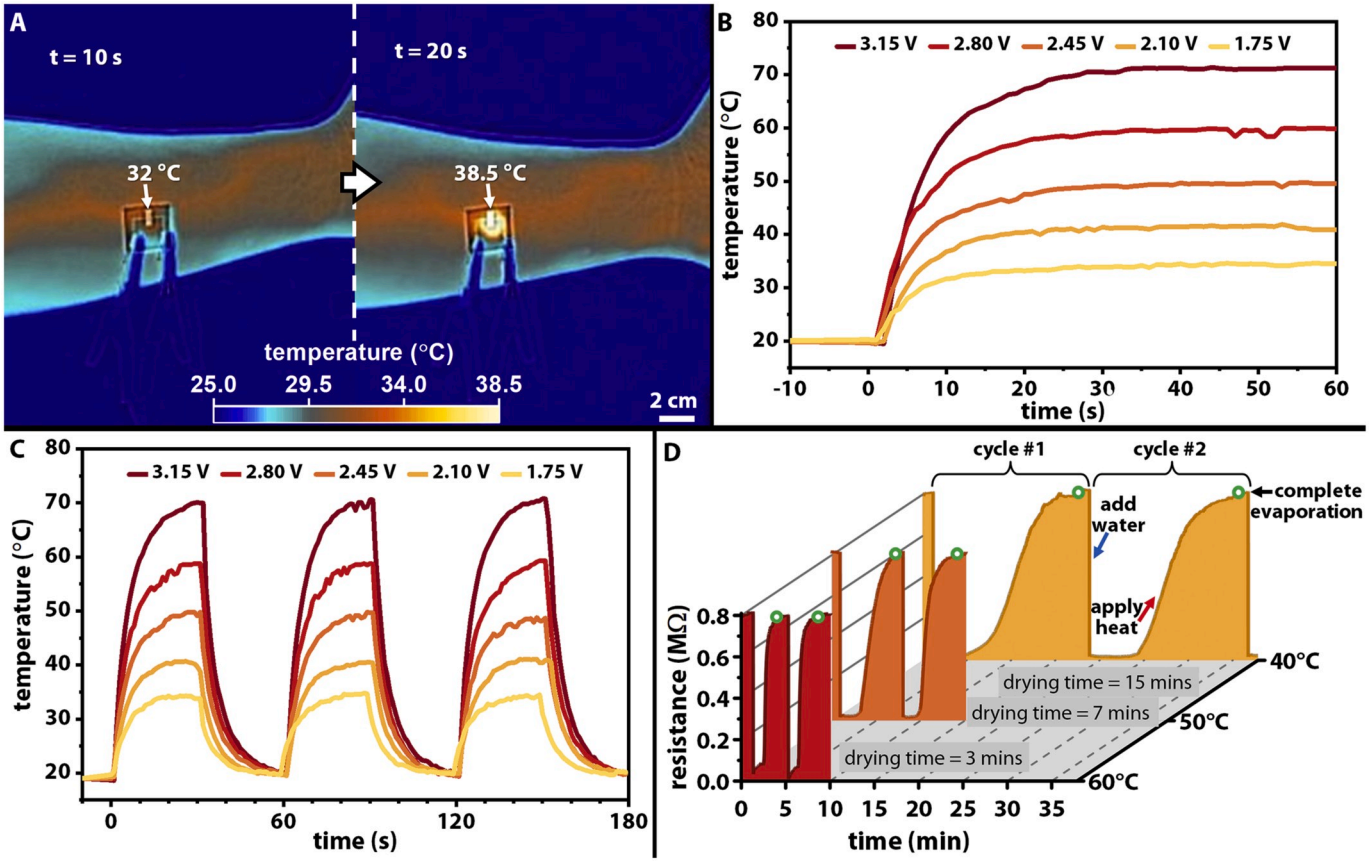

Fig. 4. Characterization of the resistive heating element in WPEDs. (A) Infrared thermography images demonstrating the use of the heating element of the WPED as a sweat stimulator by applying a constant voltage of 2.1 V. (B) Steady state temperatures achieved by the heater by applying different voltage levels (1.75 V–3.15 V). (C) Repeatability of temperatures achieved by the resistive heaters over multiple heating cycles for different voltage levels. (D) Change in resistance of the WPED as it is consecutively wetted and then dried by the resistive heating element. The drying time reduces with increase of heater temperature which is achieved by increasing the heating voltage.

paper box and this box was placed on the measuring base during 5 min. The collected measurement of vaginal pH was then wirelessly transmitted to a laptop computer through the app (Fig. 5G). After the test is performed, the paper-based container holding both the tampon and the WPED can be easily disposed, maintaining the wireless measuring stage clean.

3.6. Mechanical and thermal stability of WPEDs

WPEDs are intended to be transferred to highly deformable platforms—such as skin or cellulose-based sanitary products—to monitor pH levels. Therefore, the usability of WPEDs depends on their ability to maintain their accuracy under mechanical deformation. Fig. 6A shows the insensitivity of the analytical performance of the pH sensor to 300 loading and unloading cycles, while bending the WPED to a radius of curvature of 3 mm (Fig. 6B). The capability of WPEDs to bend to small curvatures demonstrates their suitability as wearable devices (Takei et al., 2010). Additionally, we observed minimal thermal drifts (<0.06%/°C) on the pH measurements caused by the temperature induced on the PANi/AgμFs composite by the heating element of the WPEDs (Fig. 6C and D). The thermal stability of the PANi/AgμFs pH sensor spans over the range 20–80 °C. This demonstrates that the application of heat to induce sweat or dry the pH sensor (40 °C on skin, 60 °C on tampons) does not compromise the accuracy of WPEDs.

4. Conclusions

In summary, this work reports the low-cost fabrication of highly conformal, waterproof electronic decals (WPEDs) that can be easily mounted on skin or on the surface of paper-based sample containers to monitor sweat and vaginal pH. The sensing layer of the WPEDs consists of a pH sensitive PANi/AgμFs composite whose impedance range minimizes thermal drift. Additionally, the impedance of this PANi/AgμFs composite matches the low currents typically provided by low-power wearable electronics, exhibiting a pH sensitivity of 0.407 log(Ω)/pH. An independent resistive heating element on top of the PANi/AgμFs composite serves to first stimulate sweating (for sweat pH monitoring WPEDs) and then evaporate excess of fluid in the PANi/AgμFs composite, avoiding short-circuits and reducing the variability of the measurements. WPEDs have five significant advantages over previously reported sweat pH sensors: (i) The flexibility, low thickness, and self-adhesive behavior of WPEDs facilitate their conforming to curved and irregular substrates, eliminating the somatosensory perception of these electronic decals when mounted on skin; (ii) the decoupling between the disposable WPEDs and a reusable wireless impedance analyzer with integrated data processing and transmission modules, enables the use of WPED as single-use biosensors at the point of care. A user-friendly mobile App receives, displays, encrypts, and stores the results of the pH measurements, informing the patient and transferring the data to relevant care givers so that they can provide early preventive treatment; (iii) the transparency and the breathability of WPEDs makes them barely perceptible and prevent skin irritation even when the same sensor is worn on skin for up to 3 h; (iv) the lamination of the contact pads, and the sensing and stimulating elements of the WPED with biocompatible polymers prevents metals from contacting the skin of sensitized users, further minimizing skin irritation; (v) WPEDs are moisture-insensitive

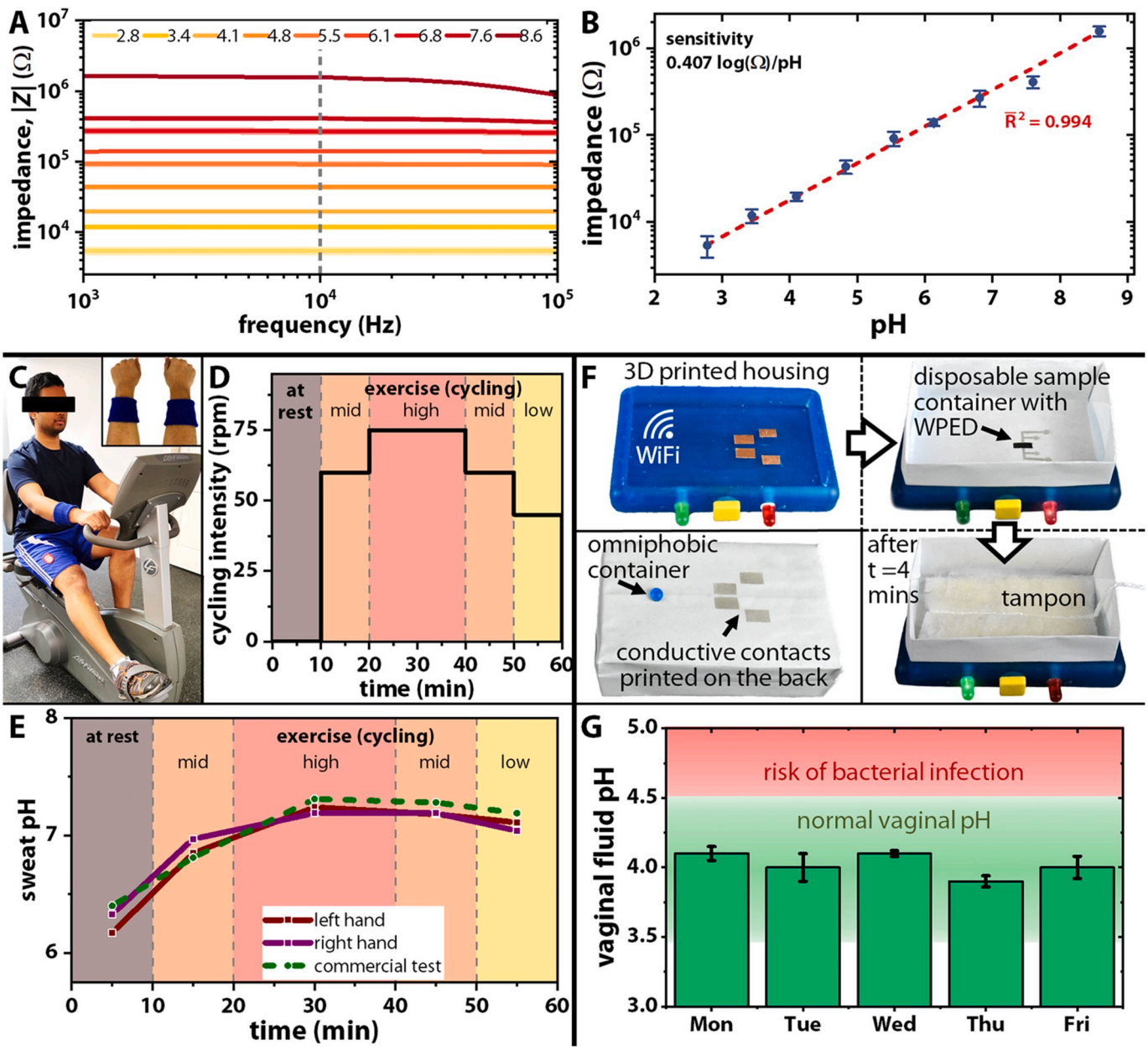

Fig. 5. Monitoring pH of sweat and vaginal fluid using WPEDs. (A) Bode plot for the magnitude of impedance measured by a WPED for pH levels of different buffers. The measured impedance is approximately constant across the frequency range of 1 kHz–10 kHz. (B) Dependence of the modulus of the impedance of the PANi/AgμFs composite on pH. The calibration curve is obtained at a 10 kHz frequency, providing a sensitivity of 0.407 log(Ω)/pH with $\overline{R}^2$ = 0.994. Error bars indicate standard deviation from 3 samples. (C) A volunteer exercising on a stationary bicycle with two WPEDs with wearable impedance analyzers worn on both forearms to monitor sweat pH. (D) Exercise intensity of the volunteer over 1 h. (E) Sweat pH values obtained from the volunteer over different phases of exercise intensity. (F) Portable WPED-based device for the at-home monitoring of vaginal pH. (G) pH of vaginal fluid of a volunteer measured over 5 consecutive days.

and exhibit high thermal and mechanical stability, conforming to the natural motions of the wearer in a variety of environments and avoiding the Nernstian thermal drift commonly observed in potentiometric pH sensors. The reported WPEDs and the wearable and portable impedance analyzers, at their present level of development, also have two limitations: (i) A measuring time of ~15 min is required to measure sweat pH at rest as the heater is limited to 42 °C, the maximum temperature which can be safely applied to the skin of the user (Zhang et al., 2017); (ii) when using WPEDs to identify vaginal infections during menstrual periods, it needs to be taken into account that the presence of blood (pH ~7.4) will naturally increase the pH of vaginal fluid. WPEDs, however, are simple to apply and to interface and can allow the accurate wireless monitoring of pH over the clinical range of a variety of biofluids such as sweat, vaginal fluid, wound exudate, or gastroesophageal reflux. We expect that WPEDs, with further development, will be able to expand the sensing capabilities of sanitary products (such as pads, tampons, or diapers) in home environments and at the point of care, and also be useful in various industrial applications, such as monitoring food and dairy quality.

Declaration of competing interest

The authors declare that they have no known competing financial interests or personal relationships that could have appeared to influence the work reported in this paper.

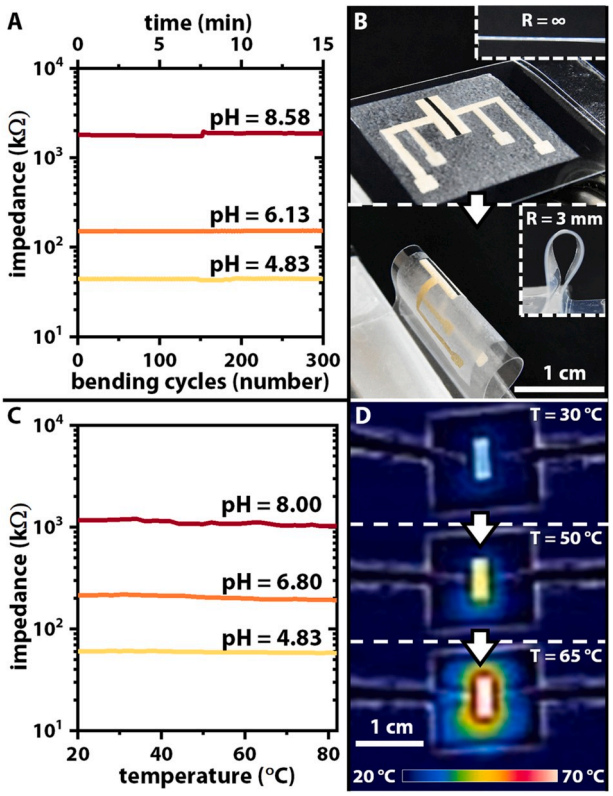

Fig. 6. Mechanical and thermal stability of the pH measurements collected using WPEDs. (A) Mechanical stability of the pH sensors at three different pH values over 300 bending cycles. (B) Bending test positions, cycling from a flat configuration to a radius of curvature of 3 mm. (C) Effect of temperature variation on the pH response of WPED at three different pH values. (D) TIR images showing the temperature of the WPED as it is heated by the heater.

CRediT authorship contribution statement

Aniket Pal: Conceptualization, Validation, Investigation, Software, Writing - original draft, Writing - review & editing, Visualization. **Vinayak G. Nadiger:** Investigation. **Debkalpa Goswami:** Investigation, Writing - review & editing, Visualization. **Ramses V. Martinez:** Conceptualization, Investigation, Writing - review & editing, Supervision, Project administration.

Acknowledgements

The authors gratefully acknowledge start-up funding from Purdue University and funding from the Indiana Clinical and Translational Sciences Institute (grant CTSI-40002729). D. G. thanks the Ross Fellowship program at Purdue University for providing partial support of his work.

Appendix A. Supplementary data

Supplementary data to this article can be found online at https://doi.org/10.1016/j.bios.2020.112206.

References

Bandodkar, A.J., Hung, V.W.S., Jia, W., Valdés-Ramírez, G., Windmiller, J.R., Martinez, A.G., Ramírez, J., Chan, G., Kerman, K., Wang, J., 2013. Tattoo-based potentiometric ion-selective sensors for epidermal pH monitoring. Analyst 138, 123–128. https://doi.org/10.1039/c2an36422k.

Bandodkar, A.J., Jia, W., Wang, J., 2015. Tattoo-based wearable electrochemical devices: a review. Electroanalysis 27, 562–572. https://doi.org/10.1002/elan.201400537.

Bariya, M., Nyein, H.Y.Y., Javey, A., 2018. Wearable sweat sensors. Nat. Electron. 1, 160–171. https://doi.org/10.1038/s41928-018-0043-y.

Benjamin, F.B., 1953. Sweating response to local heat application. J. Appl. Physiol. 5, 594–598. https://doi.org/10.1152/jappl.1953.5.10.594.

Caldara, M., Colleoni, C., Guido, E., Re, V., Rosace, G., 2016. Optical monitoring of sweat pH by a textile fabric wearable sensor based on covalently bonded litmus-3-glycidoxypropyltrimethoxysilane coating. Sensor. Actuator. B Chem. 222, 213–220. https://doi.org/10.1016/j.snb.2015.08.073.

Choi, J., Bandodkar, A.J., Reeder, J.T., Ray, T.R., Turnquist, A., Kim, S.B., Nyberg, N., Hourlier-Fargette, A., Model, J.B., Aranyosi, A.J., Xu, S., Ghaffari, R., Rogers, J.A., 2019. Soft, skin-integrated multifunctional microfluidic systems for accurate colorimetric analysis of sweat biomarkers and temperature. ACS Sens. 4, 379–388. https://doi.org/10.1021/acssensors.8b01218.

Desax, M.C., Ammann, R.A., Hammer, J., Schoeni, M.H., Barben, J., 2008. Nanoduct® sweat testing for rapid diagnosis in newborns, infants and children with cystic fibrosis. Eur. J. Pediatr. https://doi.org/10.1007/s00431-007-0485-0.

Fay, C., Barry, C., Hughes, S., Moyna, N., Curto, V.F., Diamond, D., O'Toole, C., Coyle, S., Byrne, R., Benito-Lopez, F., 2012. Real-time sweat pH monitoring based on a wearable chemical barcode micro-fluidic platform incorporating ionic liquids. Sensor. Actuator. B Chem. 171–172, 1327–1334. https://doi.org/10.1016/j.snb.2012.06.048.

Frazzoni, M., de Bortoli, N., Frazzoni, L., Tolone, S., Savarino, V., Savarino, E., 2017. Impedance-pH monitoring for diagnosis of reflux disease: new perspectives. Dig. Dis. Sci. 62, 1881–1889. https://doi.org/10.1007/s10620-017-4625-8.

Gao, W., Emaminejad, S., Nyein, H.Y.Y., Challa, S., Chen, K., Peck, A., Fahad, H.M., Ota, H., Shiraki, H., Kiriya, D., Lien, D.H., Brooks, G.A., Davis, R.W., Javey, A., 2016. Fully integrated wearable sensor arrays for multiplexed in situ perspiration analysis. Nature 529, 509–514. https://doi.org/10.1038/nature16521.

Guinovart, T., Valdés-Ramírez, G., Windmiller, J.R., Andrade, F.J., Wang, J., 2014. Bandage-based wearable potentiometric sensor for monitoring wound pH. Electroanalysis 26, 1345–1353. https://doi.org/10.1002/elan.201300558.

Hemalatha, R., Ramalaxmi, B.A., Swetha, E., Balakrishna, N., Mastromarino, P., 2013. Evaluation of vaginal pH for detection of bacterial vaginosis. Indian J. Med. Res. 138, 354–359.

Huang, W.D., Cao, H., Deb, S., Chiao, M., Chiao, J.C., 2011. A flexible pH sensor based on the iridium oxide sensing film. Sens. Actuator A Phys. 169, 1–11. https://doi.org/10.1016/j.sna.2011.05.016.

Kassal, P., Steinberg, M.D., Steinberg, I.M., 2018. Wireless chemical sensors and biosensors: a review. Sensor. Actuator. B Chem. 266, 228–245. https://doi.org/10.1016/j.snb.2018.03.074.

Khandalavala, J., Van Geem, T.A., 1999. Evaluating vaginal pH. Accuracy of two commercial pH papers in comparison to a hand-held digital pH meter. J. Reprod. Med. 44, 76–80.

King, T.L., Brucker, M.C., 2010. Pharmacology for Women's Health. Jones & Bartlett Publishers.

Koh, A., Kang, D., Xue, Y., Lee, S., Pielak, R.M., Kim, J., Hwang, T., Min, S., Banks, A., Bastien, P., Manco, M.C., Wang, L., Ammann, K.R., Jang, K.-I., Won, P., Han, S., Ghaffari, R., Paik, U., Slepian, M.J., Balooch, G., Huang, Y., Rogers, J.A., 2016. A soft, wearable microfluidic device for the capture, storage, and colorimetric sensing of sweat. Sci. Transl. Med. 8 https://doi.org/10.1126/scitranslmed.aaf2593, 366ra165.

La Belle, J.T., Adams, A., Lin, C.-E., Engelschall, E., Pratt, B., Cook, C.B., 2016. Self-monitoring of tear glucose: the development of a tear based glucose sensor as an alternative to self-monitoring of blood glucose. Chem. Commun. 52, 9197–9204. https://doi.org/10.1039/C6CC03609K.

Lee, H.-T., Liao, C.-S., Chen, S.-A., 1993. Conductivity relaxation of polyaniline. Die Makromol. Chemie Macromol. Chem. Phys. 194, 2443–2452. https://doi.org/10.1002/macp.1993.021940903.

McDonald, J.C., Duffy, D.C., Anderson, J.R., Chiu, D.T., Wu, H., Schueller, O.J.A., Whitesides, G.M., 2000. Fabrication of microfluidic systems in poly (dimethylsiloxane). Electrophoresis 21, 27–40. https://doi.org/10.1002/(SICI)1522-2683(20000101)21:1<27::AID-ELPS27>3.0.CO;2-C.

Montain, S.J., Cheuvront, S.N., Lukaski, H.C., 2007. Sweat mineral-element responses during 7 h of exercise-heat stress. Int. J. Sport Nutr. Exerc. Metabol. 17, 574–582. https://doi.org/10.1123/ijsnem.17.6.574.

Morris, D., Coyle, S., Wu, Y., Lau, K.T., Wallace, G., Diamond, D., 2009. Bio-sensing textile based patch with integrated optical detection system for sweat monitoring. Sensor. Actuator. B Chem. 139, 231–236. https://doi.org/10.1016/j.snb.2009.02.032.

Niarchos, G., Dubourg, G., Afroudakis, G., Georgopoulos, M., Tsouti, V., Makarona, E., Crnojevic-Bengin, V., Tsamis, C., 2017. Humidity sensing properties of paper substrates and their passivation with ZnO nanoparticles for sensor applications. Sensors 17, 516. https://doi.org/10.3390/s17030516.

Novell, M., Parrilla, M., Crespo, G.A., Rius, F.X., Andrade, F.J., 2012. Paper-based ion-selective potentiometric sensors. Anal. Chem. 84, 4695–4702. https://doi.org/10.1021/ac202979j.

Nyein, H.Y.Y., Gao, W., Shahpar, Z., Emaminejad, S., Challa, S., Chen, K., Fahad, H.M., Tai, L.-C., Ota, H., Davis, R.W., Javey, A., 2016. A wearable electrochemical platform for noninvasive simultaneous monitoring of Ca 2+ and pH. ACS Nano 10, 7216–7224. https://doi.org/10.1021/acsnano.6b04005.

Ochoa, M., Rahimi, R., Ziaie, B., 2014. Flexible sensors for chronic wound management. IEEE Rev. Biomed. Eng. 7, 73–86. https://doi.org/10.1109/RBME.2013.2295817.

Oh, S.Y., Hong, S.Y., Jeong, Y.R., Yun, J., Park, H., Jin, S.W., Lee, G., Oh, J.H., Lee, H., Lee, S.-S., Ha, J.S., 2018. Skin-attachable, stretchable electrochemical sweat sensor for glucose and pH detection. ACS Appl. Mater. Interfaces 10, 13729–13740. https://doi.org/10.1021/acsami.8b03342.

Pal, A., Cuellar, H.E., Kuang, R., Caurin, H.F.N., Goswami, D., Martinez, R.V., 2017. Self-powered, paper-based electrochemical devices for sensitive point-of-care testing. Adv. Mater. Technol. 2, 1700130. https://doi.org/10.1002/admt.201700130.

Pal, A., Goswami, D., Cuellar, H.E., Castro, B., Kuang, S., Martinez, R.V., 2018. Early detection and monitoring of chronic wounds using low-cost, omniphobic paper-based smart bandages. Biosens. Bioelectron. 117, 696–705. https://doi.org/10.1016/j.bios.2018.06.060.

Parrilla, M., Cánovas, R., Jeerapan, I., Andrade, F.J., Wang, J., 2016. A textile-based stretchable multi-ion potentiometric sensor. Adv. Healthc. Mater. 5, 996–1001. https://doi.org/10.1002/adhm.201600092.

Patterson, M.J., Galloway, S.D.R., Nimmo, M.A., 2002. Effect of induced metabolic alkalosis on sweat composition in men. Acta Physiol. Scand. https://doi.org/10.1046/j.1365-201x.2002.00927.x.

Pearse, A.G.E., 1968. Histochemistry: Theoretical and Applied, third ed. J. & A. Churchill Ltd., London.

Pietrzak, K., Gutarowska, B., Machnowski, W., Mikołajczyk, U., 2016. Antimicrobial properties of silver nanoparticles misting on cotton fabrics. Textil. Res. J. 86, 812–822. https://doi.org/10.1177/0040517515596933.

Rahimi, R., Ochoa, M., Parupudi, T., Zhao, X., Yazdi, I.K., Dokmeci, M.R., Tamayol, A., Khademhosseini, A., Ziaie, B., 2016. A low-cost flexible pH sensor array for wound assessment. Sensor. Actuator. B Chem. 229, 609–617. https://doi.org/10.1016/j.snb.2015.12.082.

Rahimi, R., Ochoa, M., Tamayol, A., Khalili, S., Khademhosseini, A., Ziaie, B., 2017. Highly stretchable potentiometric pH sensor fabricated via laser carbonization and machining of Carbon−Polyaniline composite. ACS Appl. Mater. Interfaces 9, 9015–9023. https://doi.org/10.1021/acsami.6b16228.

Rose, C., Parker, A., Jefferson, B., Cartmell, E., 2015. The characterization of feces and urine: a review of the literature to inform advanced treatment technology. Crit. Rev. Environ. Sci. Technol. 45, 1827–1879. https://doi.org/10.1080/10643389.2014.1000761.

Sala de Medeiros, M., Chanci, D., Moreno, C., Goswami, D., Martinez, R.V., 2019. Waterproof, breathable, and antibacterial self-powered e-textiles based on omniphobic triboelectric nanogenerators. Adv. Funct. Mater. 29, 1904350. https://doi.org/10.1002/adfm.201904350.

Schmid-Wendtner, M.H., Korting, H.C., 2006. The pH of the skin surface and its impact on the barrier function. Skin Pharmacol. Physiol. https://doi.org/10.1159/000094670.

Singh, R., Arora, V., Tandon, R., Mansingh, A., Chandra, S., 1999. Dielectric spectroscopy of doped polyaniline. Synth. Met. 104, 137–144. https://doi.org/10.1016/S0379-6779(99)00043-0.

Soares, B.G., Leyva, M.E., Barra, G.M.O., Khastgir, D., 2006. Dielectric behavior of polyaniline synthesized by different techniques. Eur. Polym. J. 42, 676–686. https://doi.org/10.1016/j.eurpolymj.2005.08.013.

Sonner, Z., Wilder, E., Heikenfeld, J., Kasting, G., Beyette, F., Swaile, D., Sherman, F., Joyce, J., Hagen, J., Kelley-Loughnane, N., Naik, R., 2015. The microfluidics of the eccrine sweat gland, including biomarker partitioning, transport, and biosensing implications. Biomicrofluidics 9, 031301. https://doi.org/10.1063/1.4921039.

Sukitpaneenit, P., Thanpitcha, T., Sirivat, A., Weder, C., Rujiravanit, R., 2007. Electrical conductivity and mechanical properties of polyaniline/natural rubber composite fibers. J. Appl. Polym. Sci. 106, 4038–4046. https://doi.org/10.1002/app.27101.

Sun, K.-H., Liu, Z., Liu, Changjian, Yu, T., Shang, T., Huang, C., Zhou, M., Liu, Cheng, Ran, F., Li, Y., Shi, Y., Pan, L., 2016. Evaluation of in vitro and in vivo biocompatibility of a myo-inositol hexakisphosphate gelated polyaniline hydrogel in a rat model. Sci. Rep. 6, 23931. https://doi.org/10.1038/srep23931.

Takei, K., Takahashi, T., Ho, J.C., Ko, H., Gillies, A.G., Leu, P.W., Fearing, R.S., Javey, A., 2010. Nanowire active-matrix circuitry for low-voltage macroscale artificial skin. Nat. Mater. 9, 821–826. https://doi.org/10.1038/nmat2835.

Wingo, J.E., Low, D.A., Keller, D.M., Brothers, R.M., Shibasaki, M., Crandall, C.G., 2010. Skin blood flow and local temperature independently modify sweat rate during passive heat stress in humans. J. Appl. Physiol. 109, 1301–1306. https://doi.org/10.1152/japplphysiol.00646.2010.

Wu, E., Chen, K., Shahpar, Z., Milla, C., Challa, S., Davis, R.W., Emaminejad, S., Javey, A., Fahad, H.M., Ryan, S.P., Davies, Z.A., Gao, W., Yin Yin Nyein, H., Talebi, S., 2017. Autonomous sweat extraction and analysis applied to cystic fibrosis and glucose monitoring using a fully integrated wearable platform. Proc. Natl. Acad. Sci. Unit. States Am. 114, 4625–4630. https://doi.org/10.1073/pnas.1701740114.

Yao, H., Shum, A.J., Cowan, M., Lähdesmäki, I., Parviz, B.A., 2011. A contact lens with embedded sensor for monitoring tear glucose level. Biosens. Bioelectron. 26, 3290–3296. https://doi.org/10.1016/J.BIOS.2010.12.042.

Zhang, Q., Murawsky, M., LaCount, T., Hao, J., Kasting, G.B., Newman, B., Ghosh, P., Raney, S.G., Li, S.K., 2017. Characterization of temperature profiles in skin and transdermal delivery system when exposed to temperature gradients in vivo and in vitro. Pharm. Res. (N. Y.) 34, 1491–1504. https://doi.org/10.1007/s11095-017-2171-x.